THE JOURNAL OF BIOLOGICAL CHEMISTRY
Vol. 280, No. 1, Issue of January 7, pp. 738–744, 2005
Printed in U.S.A.
© 2005 by The American Society for Biochemistry and Molecular Biology, Inc.

Crystal Structure of Mouse Carnitine Octanoyltransferase and Molecular Determinants of Substrate Selectivity*[S]

Received for publication, August 27, 2004, and in revised form, October 4, 2004
Published, JBC Papers in Press, October 17, 2004, DOI 10.1074/jbc.M409894200

Gerwald Jogl, Yu-Shan Hsiao, and Liang Tong‡

From the Department of Biological Sciences, Columbia University, New York, New York 10027

Carnitine acyltransferases have crucial functions in fatty acid metabolism. Members of this enzyme family show distinctive substrate preferences for short-, medium- or long-chain fatty acids. The molecular mechanism for this substrate selectivity is not clear as so far only the structure of carnitine acetyltransferase has been determined. To further our understanding of these important enzymes, we report here the crystal structures at up to 2.0-Å resolution of mouse carnitine octanoyltransferase alone and in complex with the substrate octanoylcarnitine. The structures reveal significant differences in the acyl group binding pocket between carnitine octanoyltransferase and carnitine acetyltransferase. Amino acid substitutions and structural changes produce a larger hydrophobic pocket that binds the octanoyl group in an extended conformation. Mutation of a single residue (Gly-553) in this pocket can change the substrate preference between short- and medium-chain acyl groups. The side chains of Cys-323 and Met-335 at the bottom of this pocket assume dual conformations in the substrate complex, and mutagenesis studies suggest that the Met-335 residue is important for catalysis.

Carnitine acyltransferases catalyze the reversible transfer of acyl groups between carnitine and coenzyme A (see Fig. 1*A*) (1–4). Members of this family of enzymes include carnitine palmitoyltransferases (CPTs)[1] I and II (CPT-I, CPT-II), carnitine octanoyltransferase (CrOT), and carnitine acetyltransferase (CrAT) with substrate preferences for long-chain, medium-chain, and short-chain acyl groups, respectively. The catalytic domains of these enzymes contain about 600 amino acid residues (see Fig. 1*B*), and share ~30% amino acid sequence identity (see supplemental Fig. 1).

Carnitine acyltransferases are of crucial importance for the transport of fatty acids among different cellular compartments (2–4). The CPTs are associated with the mitochondrial compartment and are essential for the import of long-chain fatty acids into the mitochondria for β-oxidation. The CoA esters of long-chain fatty acids are impermeable to the mitochondrial membrane. They must first be converted to carnitine esters by CPT-I, which is integrally associated with the outer membrane of the mitochondria through a unique N-terminal segment (see Fig. 1*B*) (5). Upon transport into the mitochondria, the carnitine esters are converted back to CoA esters by CPT-II, which is located in the mitochondrial matrix. The CoA esters can then undergo β-oxidation for energy production.

The CPTs are therefore key enzymes for the transport of long-chain fatty acids. Inherited mutational defects of these enzymes are the cause of many human diseases (2, 3). CPT-I deficiency is linked to serious episodes of hypoketonic hypoglycemia, whereas autosomal recessive deficiency of CPT-II is one of the most common inherited muscle lipid metabolism disorders (6). Both missense and deletion mutations have been described for these enzymes, and the defect of the mutated enzymes is most often caused by their reduced catalytic activity.

The CPTs are promising targets for drug development against several important human diseases (3, 7–9). An irreversible inhibitor of CPT-I can reduce blood glucose levels in diabetic animals and humans, validating this enzyme as a target for the treatment of type 2 diabetes. More recently, an agonist of CPT-I has been shown to stimulate fatty acid oxidation and reduce body weight in test animals, suggesting that such compounds may be efficacious against obesity (10, 11). Unfortunately, the currently known modulators of CPT-I have rather poor pharmacokinetic properties, and new classes of compounds need to be identified. However, this process is hampered by the relative lack of structural information on these enzymes.

CrOT (EC 2.3.1.137) contains 612 amino acid residues (Fig. 1*B*) and is localized in the peroxisomes (12, 13). It is most active for substrates with a chain length between 6 and 10 carbon atoms and is less active with substrates containing 12 to 16 carbon atoms (14). The β-oxidation of very long-chain and branched-chain fatty acids occurs in the peroxisomes. The medium- and short-chain CoA esters produced by peroxisomal β-oxidation are converted to carnitine esters by CrOT and peroxisomal CrAT, allowing their export to the cytosol and ultimately the mitochondria where they can undergo the final steps of β-oxidation (13, 15). In addition to the peroxisomes, CrAT is also found in the mitochondria, where it may have a role in maintaining the acetyl-CoA:CoA balance.

We have recently reported the crystal structures of mouse CrAT, alone and in complex with its substrate carnitine or CoA (16, 17). Crystal structures of human CrAT, alone or in complex with carnitine (18, 19), as well as choline acetyltransferase (20), have also been reported. These studies reveal that carnitine acyltransferases contain two structural domains, N and C domains, that unexpectedly share the same backbone fold with each other and with that of chloramphenicol acetyltransferase (21). The active site of the enzyme is located at the interface of the two domains, accessible from the surface of the enzyme

* This research is supported in part by National Institutes of Health Grant DK67238 (to L. T.). The costs of publication of this article were defrayed in part by the payment of page charges. This article must therefore be hereby marked "*advertisement*" in accordance with 18 U.S.C. Section 1734 solely to indicate this fact.

The atomic coordinates and structure factors (code 1XL7, 1XL8, 1XMC, 1XMD) have been deposited in the Protein Data Bank, Research Collaboratory for Structural Bioinformatics, Rutgers University, New Brunswick, NJ (http://www.rcsb.org/).

[S] The on-line version of this article (available at http://www.jbc.org) contains supplemental Figs. 1–3.

‡ To whom correspondence should be addressed. Tel.: 212-854-5203; Fax: 212-854-5207; E-mail: tong@como.bio.columbia.edu.

[1] The abbreviations used are: CPT, carnitine palmitoyltransferase; CrOT, carnitine octanoyltransferase; CrAT, carnitine acetyltransferase; r.m.s., root mean square.

Supplemental Material can be found at:
http://www.jbc.org/cgi/content/full/M409894200/DC1
This paper is available on line at http://www.jbc.org

Downloaded from www.jbc.org by on August 19, 2006

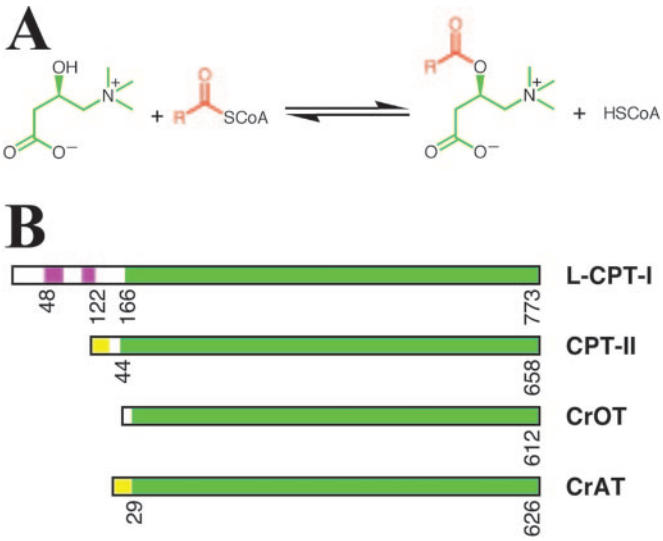

FIG. 1. **The carnitine acyltransferases.** *A*, the reaction catalyzed by carnitine acyltransferases. *B*, domain organization of representative carnitine acyltransferases, human liver-type carnitine palmitoyltransferase I (L-CPT-I), human CPT-II, mouse CrOT, and mouse CrAT. *Green*, catalytic domain; *yellow*, mitochondrial targeting sequence; *magenta*, transmembrane segment.

through two tunnels. The structural analyses suggest that the Met564 residue of CrAT may block the entrance to the acyl group binding site, limiting the substrate preference of this enzyme to short-chain acyl groups. Mutagenesis and structural studies confirm the importance of this residue in determining substrate selectivity of CrAT such that the M564G single-site mutant has significantly enhanced activity toward medium-chain acyl groups (22, 23).

We report here the crystal structures of mouse CrOT, alone and in complex with the substrate octanoylcarnitine, at up to 2.0-Å resolution. This is the first time that the binding mode of an acyl group to the carnitine acyltransferases has been observed experimentally. The overall structure of CrOT is remarkably similar to that of CrAT, and the two enzymes share 36% amino acid sequence identity. Significant differences are observed however in the acyl group binding site of the two enzymes. Amino acid substitutions together with structural differences between the two enzymes help define the binding site for medium-chain acyl groups in CrOT. Our structures show that a methionine residue at the bottom of the octanoyl binding site assumes dual conformations in the complex with octanoylcarnitine, and mutagenesis studies show that this residue is important for the catalytic activity of the enzyme.

MATERIALS AND METHODS

Protein Expression and Purification—Full-length mouse CrOT was sub-cloned into the pET28a vector (Novagen) and over-expressed in *Escherichia coli*. The expression construct introduced a hexahistidine tag at the C terminus of the protein. The soluble protein was purified by nickel-agarose affinity chromatography, anion exchange, and gel filtration chromatography. The protein was concentrated to 20 mg/ml in a buffer containing 20 mM Tris (pH 8.5) and 20 mM NaCl and stored at −80 °C. The C-terminal His tag was not removed for crystallization.

For the production of selenomethionyl protein, the expression construct was transformed into B834(DE3) cells. The bacterial growth was carried out in defined LeMaster media (24), and the protein was purified using the same protocol as for the wild-type protein.

Protein Crystallization—Small crystals of the free enzyme of mouse CrOT were obtained at 4 °C by the sitting drop vapor diffusion method. The reservoir solution contained 100 mM Hepes (pH 7.4) and 62% (v/v) 2-methyl-2,4-pentanediol. Larger crystals were grown from the same condition by microseeding followed by macroseeding. Selenomethionine-labeled protein was cross-seeded with microcrystals from native protein to obtain adequate crystals. For data collection, crystals were flash-frozen in liquid nitrogen directly in the mother liquor.

To determine the binding mode of the octanoylcarnitine substrate by soaking experiments, the free enzyme crystals were first soaked in a Tris-buffered solution to remove the Hepes molecule that was observed in the active site. Crystals in the Tris buffer were soaked with octanoylcarnitine for various lengths of time. It was discovered that the acylcarnitine was rapidly hydrolyzed by the enzyme, and we invariably observed only the binding of carnitine to the active site if the soaking time was longer than 20 min. From a 5-min soaking experiment, we were able to observe the binding of octanoylcarnitine to one of the two molecules in the asymmetric unit, whereas the other molecule contained carnitine.

Data Collection and Processing—X-ray diffraction data were collected on an ADSC charge-coupled device at the X4A beamline of Brookhaven National Laboratory. A selenomethionyl single-wavelength anomalous diffraction data set to 2.0-Å resolution was collected at 100 K on a crystal of the free enzyme, and a native reflection data set to 2.2-Å resolution was collected for the octanoylcarnitine soak. The diffraction images were processed and scaled with the HKL package (25). The crystals belong to the space group $R3$, with cell dimensions of $a = b = 162.6$ Å and $c = 158.6$ Å for the free enzyme. There are two molecules of CrOT in the crystallographic asymmetric unit. The data processing statistics are summarized in Table I.

Structure Determination and Refinement—The locations of 34 selenium atoms were determined with the program SnB (26) and further confirmed with SHELXS (27). Reflection phases to 1.8-Å resolution were calculated based on the single-wavelength anomalous diffraction data and improved with the program SOLVE (28), which also automatically located a significant portion of the residues in both molecules. The atomic model was fit into the electron density with the program O (29). The structure refinement was carried out with the program CNS (30). The statistics of the structure refinement are summarized in Table I.

Mutagenesis and Kinetic Studies—The mutants were designed based on the structural information, created with the QuikChange kit (Stratagene), and verified by sequencing. The substrate preference of wild-type and mutant CrOT enzymes were determined by kinetic studies following a protocol reported earlier (31). The reaction buffer contained 25 mM potassium phosphate (pH 7.4), 125 μM 4,4′-dithiobispyridine (dissolved in ethanol), 0.5 mM acyl-CoA, 2 mM carnitine, and 0.5 μg of enzyme in a volume of 0.2 ml. The reaction was monitored by the increase in absorbance at 324 nm. The assays were repeated 2–5 times for each enzyme preparation with each substrate to verify the observed reaction velocity.

Structure Determination of the M335V and C323M Mutants—The M335V and C323M mutants of CrOT were crystallized with the sitting drop vapor diffusion method using essentially the same condition as the wild-type enzyme. X-ray diffraction data were collected at the X4A beamline of the National Synchroton Light Source, and the crystals are isomorphous to those of the wild type. The data processing and structure refinement followed the same protocol as that for the wild-type enzyme of structures reported here.

Atomic Coordinates—The atomic coordinates of structures reported here were deposited in the Protein Data Bank (accession codes 1XL7, 1XL8, 1XMC, 1XMD).

RESULTS AND DISCUSSION

Structure Determination—The crystal structure of the free enzyme of mouse CrOT was solved at 2.0-Å resolution using the selenomethionyl single-wavelength anomalous diffraction method (32). There are two molecules of CrOT in the asymmetric unit of the crystal, and 34 of the expected 36 selenium positions were located from the anomalous difference data. The current atomic model has an R value of 19.0%, and the majority of the residues (92.6%) are in the most favored region of the Ramachandran plot (data not shown). The crystallographic information is summarized in Table I.

The structure of CrOT in complex with octanoylcarnitine has been determined at 2.2-Å resolution (Table I) from a crystal that was soaked with this substrate for approximately 5 min. We found that octanoylcarnitine was rapidly hydrolyzed by the crystals, and those soaked for longer times contained only carnitine in the active site (data not shown). With a soaking time of 5 min, our crystallographic analysis showed that one of the two CrOT molecules in the asymmetric unit contained octanoylcarnitine in the active site, whereas the other contained only carnitine. This

Downloaded from www.jbc.org by on August 19, 2006

TABLE I
Summary of crystallographic information

Enzyme	Wild type	Wild type	M335V mutant	C323M mutant
Substrate		Octanoyl-carnitine		
Maximum resolution (Å)	2.0	2.2	2.1	2.0
Number of observations	842,405	283,268	271,285	342,328
R_{merge} (%)[a]	9.5 (56)	9.1 (42)	8.5 (30.8)	5.2 (18.7)
Resolution range used for refinement	30–2.0 Å	30–2.2 Å	30–2.1 Å	30–2.0 Å
Number of reflections	200,189[b]	76,996	88,238	97,083
Completeness (%) (0σ cutoff)	95 (87)	95 (88)	95 (86)	90 (85)
R factor (%)[c]	19.0 (25.8)	19.0 (25.5)	19.6 (24.2)	19.0 (21.5)
Free R factor (%)	21.7 (27.7)	23.0 (29.7)	22.4 (27.0)	21.7 (25.5)
r.m.s. deviation in bond lengths (Å)	0.007	0.006	0.006	0.006
r.m.s. deviation in bond angles (°)	1.3	1.2	1.2	1.3

[a] $R_{merge} = \sum_h \sum_i |I_{hi} - \langle I_h \rangle| \Big/ \sum_h \sum_i I_{hi}$. Numbers in parentheses are for the highest resolution shell.

[b] Both Friedel mates are used in the refinement.

[c] $R = \sum_h |F_h^o - F_h^c| \Big/ \sum_h F_h^o$.

suggests that the two enzyme molecules might have different catalytic activity in the crystalline state.

In both the free enzyme and the octanoylcarnitine complex, residues 1–10 and the C-terminal hexahistidine tag are disordered. In addition, residues 403–413 have weak electron density, and these residues are not included in the atomic model for one of the two CrOT molecules.

The two CrOT molecules in the asymmetric unit have essentially the same conformation, with an r.m.s. distance between equivalent Cα atoms of 0.36 Å for the free enzyme and 0.39 Å for the octanoylcarnitine complex (calculated with LSQMAN for all Cα pairs). The intermolecular contacts between the two molecules are generally weak and hydrophilic in nature. The structural information is consistent with our observations that CrOT migrates as a monomer on the gel filtration column (data not shown). Other biochemical data also suggest a monomeric native structure for CrOT (31).

Our attempts at determining the structure of CrOT in complex with the CoA substrate have so far not been successful. Examination of the packing of the current crystal form shows that the CoA binding site is likely to be occluded by neighboring molecules in the crystal, explaining the lack of success with the soaking protocol. At the same time, we have not been able to crystallize CrOT in the presence of CoA.

Overall Structure of CrOT—The structure of CrOT consists of 20 α-helices (named α1 through α20) and 16 β-strands (β1 through β16) and can be divided into two domains, N and C domains (Fig. 2*A*). The N domain covers residues 102 to 393, whereas the C domain covers residues 394–612 together with residues 11–101 at the N terminus. The two domains have the same backbone fold with a central mixed β-sheet and several flanking helices as their common features (Fig. 2*A*). A total of 68 Cα positions can be superimposed structurally between the two domains, and the r.m.s. distance for these Cα atoms is 2.1 Å. However, the amino acid sequence identity for these structurally equivalent residues is only 9%.

The backbone fold of the two domains of CrOT is related to other acetyltransferases, especially chloramphenicol acetyltransferase (21) and the catalytic domain of dihydrolipoyl transacetylase (33) as was first observed with the structure of CrAT (16, 18). The carnitine acyltransferases may have evolved by gene duplication of a primordial, prokaryotic acetyltransferase.

The overall structure of CrOT is remarkably similar to that of CrAT (16), and the positions of the secondary structure elements are conserved in both enzymes (Fig. 2*B*). The r.m.s. distance between equivalent Cα atoms of the two structures is 1.4 Å (calculated with LSQMAN), consistent with the fact that the two enzymes share 36% amino acid sequence identity (supplemental Fig. 1) (34). However, significant differences were observed in the acyl group binding region of the active site (see below), which defines the differing substrate selectivity of these two enzymes. In addition, several loops on the surface of the N domain have large differences between the two enzymes (Fig. 2*B*).

The Carnitine Binding Site—The active site of CrOT is located at the interface of the two domains (Fig. 2*A*). The catalytic residue, His-327, is positioned near the center of the enzyme. It is accessible from opposite surfaces of the enzyme through two tunnels that meet at the active site (Fig. 3*A*) (16). One of these tunnels is for binding the carnitine substrate, whereas the other is for CoA. In the structure of CrOT, a third tunnel extends from the active site toward the core of the N domain (Fig. 3*A*). This is the tunnel for binding the medium-chain acyl group of the substrate.

In the crystal that was soaked with octanoylcarnitine, one of the CrOT molecules in the asymmetric unit has octanoylcarnitine in the active site (Fig. 3*A*), whereas the other has only carnitine. Superimposing the two protein molecules shows that the positions of carnitine are the same in the two complexes. This confirms that the presence of the acyl group does not disturb the binding of carnitine.

Next we compared the binding mode of carnitine in complex with CrOT to that in complex with CrAT (Fig. 3*B*). Although the overall binding modes of the carnitine molecules are similar, there are recognizable differences in their positions. The carboxylate group of carnitine shifts by about 0.7 Å in the CrOT complex relative to the CrAT complex (Fig. 3*B*), although the carboxylate is recognized by an equivalent set of intricate hydrogen bonding and ion pair interactions (Fig. 3*C*). Only two residues are different between CrOT and CrAT in this binding site, Asp-331 (Glu-347 in CrAT) and Thr-441 (Ser-454 in CrAT), but these differences do not affect the binding of carnitine (Fig. 3*B*).

The largest difference in the binding mode of carnitine is observed for the trimethylammonium group, which shifts by about 1.1 Å in the complex with CrOT (Fig. 3*B*). Moreover, residues that line the trimethylammonium binding pocket show large variations between CrOT and CrAT (Fig. 3*B*), including Val-555 (Phe-566 in CrAT) and Phe-566 (Cys-577 in CrAT). Interestingly, these two variations are compensatory of each other, which help to maintain the overall shape and the hydrophobic nature of the trimethylammonium binding site. The larger changes in both the position of the trimethylammonium group and in its binding pocket are consistent with the notion that this group is not bound through specific interactions with the carnitine acyltransferases and that the positive charge of this group may instead be important for stabilizing

Downloaded from www.jbc.org by on August 19, 2006

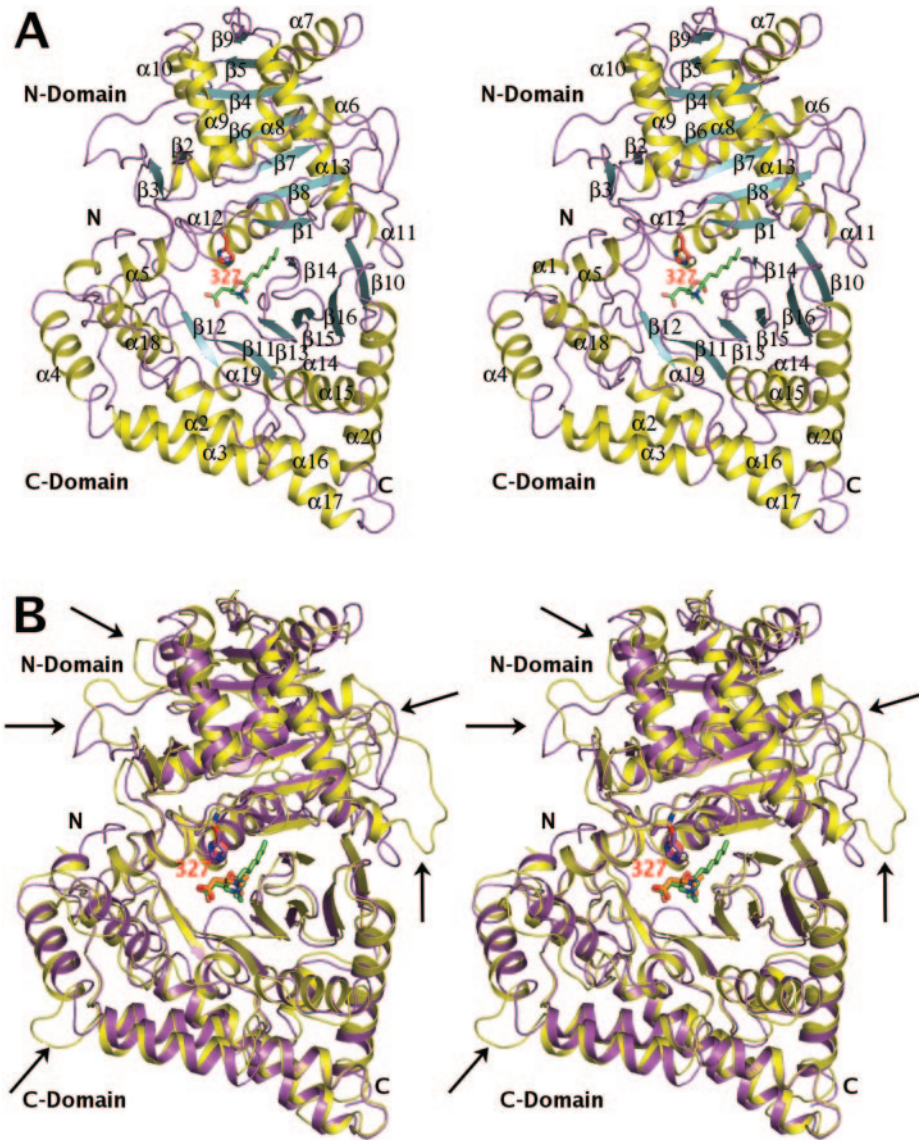

FIG. 2. **Structure of CrOT.** *A*, stereo diagram showing a schematic representation of the structure of CrOT. Secondary structure elements are labeled, and the catalytic histidine is shown in *red*. The octanoylcarnitine substrate is shown in *green*. All molecular figures were produced with Pymol (36). *B*, overall superposition of the structures of CrOT (*magenta*) and CrAT (*yellow*). Both catalytic histidine residues are shown in *red*. Carnitine from CrAT is shown in *yellow*, coenzyme A from CrAT is shown in *orange*, and octanoylcarnitine from CrOT is shown in *green*. Several loops that show large structural differences between the two enzymes are indicated with *arrows*.

the transition state of the catalysis (16).

The free enzyme crystals were grown from a solution containing Hepes and 2-methyl-2,4-pentanediol. Our crystallographic analysis showed that both molecules are bound in the active site of the enzyme. The sulfonic acid of Hepes is situated in the binding site for the carboxylate group of carnitine, suggesting that this binding site is an "anion hole" that can recognize many different types of negatively charged groups.

The Binding Site for Medium-chain Acyl Groups—Our crystallographic analysis revealed well defined electron density for the octanoylcarnitine substrate in the active site of CrOT (Fig. 4*A*). This is the first time that the binding mode of an acyl group to the carnitine acyltransferases has been observed experimentally. The acyl group has relatively weaker electron density, especially at the C7′ and C8′ positions. This may be caused by partial disorder of the end of the acyl group. Another possibility is that octanoylcarnitine is present only in partial occupancy. However, this is less likely as the average temperature factor value for the substrate (including its acyl group) is essentially the same as that for the enzyme.

The octanoyl group is bound in an extended but slightly bent conformation (Fig. 4*B*). The binding pocket is lined in its entire length with hydrophobic residues, coming from strand β1 (Phe-103, Gly-105), β8 (Cys-323, Cys-325), β13 (Ser-544), β13-β14 loop (Val-546), β14 (Val-551, Gly-553, Val-555), β15 (Phe-566), and α12 (Ala-332, Met-333, Met-335, Val-336). These residues define a narrow, cylindrical-shaped binding site (Fig. 5*A*), which represents a good fit to the contour of acyl groups.

With the exception of Met-335 and Cys-323, residues in this binding site show little conformational change between the free enzyme and the octanoylcarnitine complex, suggesting that the acyl group binding site is essentially preformed in the structure of CrOT. The side chains of Met-335 and Cys-323 assume dual conformations in the complex with octanoylcarnitine (supplemental Fig. 2*A*), whereas in the free enzyme and the carnitine complex only a single conformation is observed (supplemental Fig. 2*B*). These two side chains interact with each other and with the C8′ atom of the octanoyl group (Fig. 4*B*), and their disorder may create additional space for the octanoyl group (see below).

The carbonyl oxygen of the acyl group is pointed toward the side chain of Ser-544, although the hydroxyl group of the side chain is not positioned correctly for hydrogen bonding to the substrate (Fig. 4*B*). Ser-544 is the second serine residue in the Ser-Thr-Ser motif that is strictly conserved among the carnitine acyltransferases (supplemental Fig. 1). Structural and mutagenesis studies suggest that this side chain may help stabilize the oxyanion in the tetrahedral intermediate of the reaction (16, 35). By assuming a different rotamer, Ser-544 should be able to hydrogen bond to the oxyanion of the intermediate. At the same time, our structural analysis of CrAT

Downloaded from www.jbc.org by on August 19, 2006

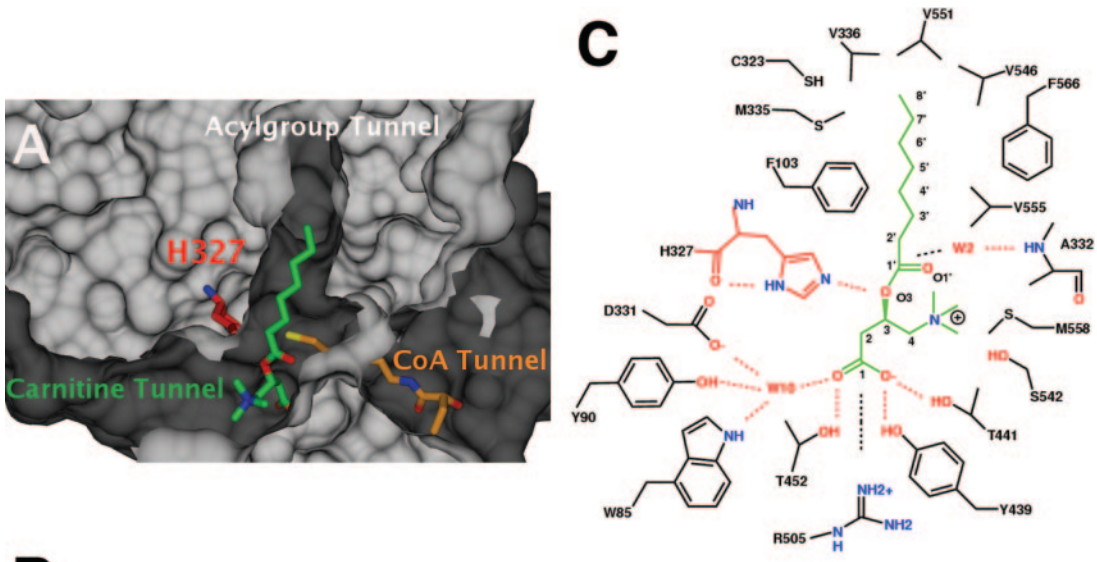

FIG. 3. **The carnitine binding site of CrOT.** *A*, the three tunnels for binding carnitine, CoA, and the acyl group in the active site of CrOT. *B*, superposition of the binding modes of carnitine to CrOT (secondary structures, *cyan*; and side chains, *blue*) and CrAT (*yellow* and *orange*). The solvent water W10, which mediates important contacts for octanoylcarnitine binding, and the solvent water W2 (close to the octanoylcarnitine carbonyl group) are shown as *red spheres*. *C*, schematic drawing of the interactions between octanoylcarnitine and CrOT. Hydrogen bonding interactions are shown in *red dashed lines*. The electrostatic interaction between the carboxylate group and Arg-505 is shown as a *black dashed line*. The close distance between the solvent water, W2, and the octanoylcarnitine C1′ is indicated with a *black dashed line*.

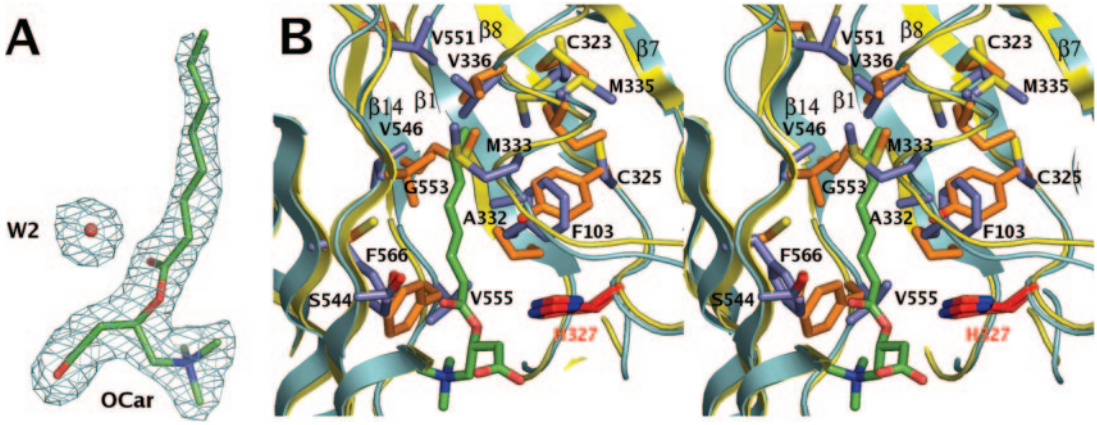

FIG. 4. **The binding mode of octanoylcarnitine.** *A*, final $2F_o - F_c$ electron density for octanoylcarnitine and the solvent water W2 close to the carbonyl group of octanoylcarnitine at 2.2-Å resolution. The contour level is 1σ. *B*, stereo representation of the octanoylcarnitine binding site in CrOT. His-327 is shown in *red*.

suggests that the trimethylammonium group of carnitine may play a more important role in stabilizing the transition state, and carnitine acyltransferases are an example of substrate assisted catalysis (16).

In the structure of CrOT in complex with octanoylcarnitine, a water molecule is located 3.2 Å from the carbonyl carbon (C1′) of the octanoyl group (Figs. 4*A* and 3*B*). This water molecule is hydrogen bonded to the main chain amide of Ala-332 (in helix

Downloaded from www.jbc.org by on August 19, 2006

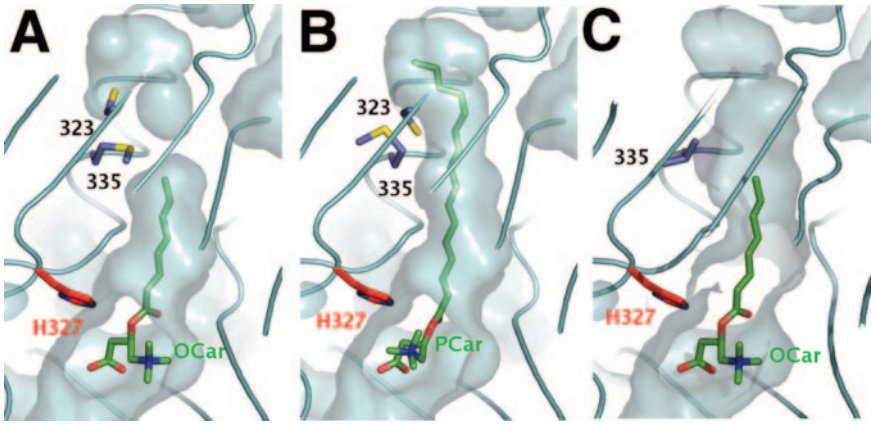

FIG. 5. **The acyl group binding site.** *A*, the acyl group binding pocket for one conformation of the Met-335 and Cys-323 residues. His-327 is shown in *red*. Met-335 is close to the substrate in this conformation. *B*, the acyl group binding pocket for the other conformation of the Met-335 and Cys-323 residues. A modeled conformation for palmitoylcarnitine (labeled *PCar*) is shown for reference. *C*, the acyl group binding pocket for the M335V mutant.

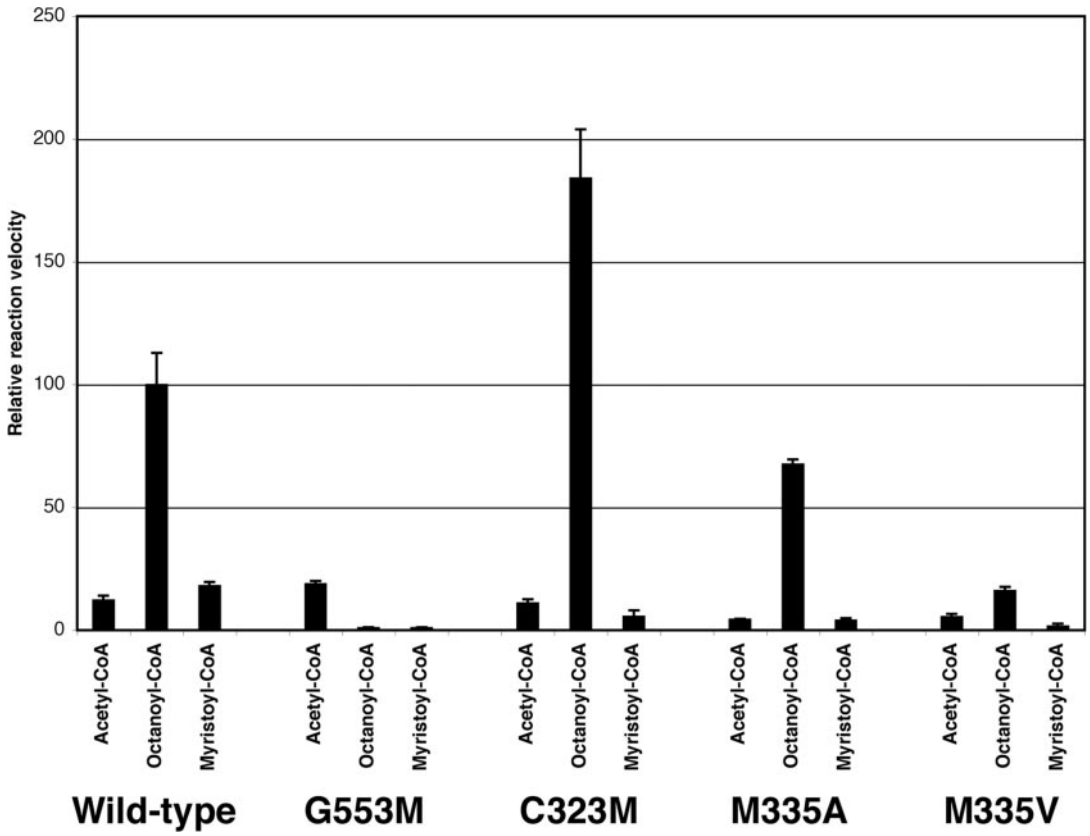

FIG. 6. **Substrate preference of wild-type and mutant CrOT enzymes.** The assay monitored the production of CoA with saturating concentrations of the acyl-CoA and carnitine substrates (31). The reaction velocity of the wild-type enzyme with the octanoyl-CoA substrate is scaled to 100. *Error bars* represent standard deviation in the measurements.

α12) (Fig. 3*C*) and is also observed in the structures of the free enzyme and the carnitine complex of CrOT. It occupies roughly the same position as the thiol group of the CoA substrate that is observed in the structure of CrAT (16). It is therefore likely that this water molecule can function as a nucleophile and initiate the hydrolysis of bound acylcarnitine substrates. This explains our observation of rapid hydrolysis of acylcarnitines during soaking experiments.

Molecular Determinants of Substrate Selectivity of CrOT and CrAT—Sequence and structural variations between CrOT and CrAT in the acyl group binding site determine their substrate preferences. Remarkably, only three of the residues (Val-336, Ser-544, Val-546) in this binding site are conserved between the two enzymes (supplemental Fig. 1). Moreover, residue Val-546 assumes a different conformation in the structure of CrOT (Fig. 4*B*) despite being conserved between the two enzymes. This conformation places its side chain further from the octanoyl group (Fig. 4*B*), thereby creating additional space in the binding site.

Sequence variations in the other residues in the binding site probably play a larger role in determining the substrate preferences of the two enzymes. Our structural analysis shows that the most important difference between CrOT and CrAT is the replacement of Gly-553 (β14) in CrOT with Met-564 in CrAT (supplemental Fig. 1). This residue is Met only in CrAT and is Gly in CrOT and also in all the CPTs (supplemental Fig. 1). The Met side chain fills the acyl group binding site and would actually clash with the octanoyl group (Fig. 4*B*). Recent studies show that the single-site M564G mutation of CrAT is sufficient to alter the substrate selectivity of that enzyme, so that hexanoyl-CoA is the preferred substrate (22, 23). These studies suggest that Met-564 in CrAT may be the "gatekeeper" to the binding site for medium- and long-chain acyl groups.

The structural, sequence, and biochemical studies therefore

Downloaded from www.jbc.org by on August 19, 2006

suggest that the G553M mutation of CrOT should be able to limit the substrate preference of CrOT to short-chain acyl groups. Our kinetic characterization of the G553M mutant of CrOT confirms the important role of Gly-553 in defining the substrate selectivity of CrOT (Fig. 6) as has also been reported in a different study (23). The G553M mutant can no longer utilize octanoyl-CoA as a substrate, although the activity with the short-chain acetyl-CoA substrate is maintained.

Additional sequence variations between CrOT and CrAT may also have an impact on the substrate selectivity of these enzymes. The side chain of Tyr-341 in CrAT is within 3.3 Å of the C4′ atom of octanoylcarnitine. This residue is replaced with Cys-325 in CrOT (supplemental Fig. 1), alleviating the contact with the octanoyl group (Fig. 4*B*). Interestingly, Phe-103 of CrOT replaces Pro-120 of CrAT, and the phenyl ring occupies part of the space vacated by the Tyr-341 side chain (Fig. 4*B*). In addition, replacement of Gly-105 in CrOT by Val-122 in CrAT may create unfavorable contacts with the C8′ atom of the octanoyl group. Finally, residues 546–552 of CrOT (β13-β14 loop) have a different conformation compared with their equivalents in CrAT (Fig. 4*B*), which also affects the binding site near the C8′ atom.

Functional Relevance of the Disordering of the Met-335 and Cys-323 Side Chains—Our structural analysis shows that the side chains of Met-335 and Cys-323 assume dual conformations in the complex with octanoylcarnitine. The two conformations of Met-335 are distinguished by the placement of the SD and CE atoms in its side chain. In one conformation, these atoms are located closer to the C8′ atom of octanoylcarnitine (Fig. 4*B*), whereas they are swung away in the other conformation. It is likely that the dual conformation in the side chain of Cys-323 is induced by that of Met-335, as the two side chains are in direct contact with each other (Fig. 4*B*).

What is the functional role, if any, for the disordering of these two residues? Molecular surface analysis suggests that when the Met-335 side chain is further from the octanoyl group, a larger acyl group binding pocket could be formed, which might allow the enzyme to utilize longer fatty acids as substrates (Fig. 5*B*). Interestingly, this Met residue is replaced by a smaller Val residue in the CPTs (supplemental Fig. 1), which also suggests that this residue might control access by the long-chain substrates.

To assess the functional relevance of these residues, we have created single-site mutants of CrOT, replacing Met-335 with Val (M335V mutant) or Ala (M335A), as well as replacing Cys-323 with Met (C323M mutant). The C323M mutant was chosen because the equivalent residue of Cys-323 in CrAT is Met (supplemental Fig. 1). The kinetic data show that the C323M mutant has slightly higher catalytic activity with the octanoyl-CoA substrate but maintains the same substrate preference as the wild-type enzyme (Fig. 6). Somewhat unexpectedly, our kinetic experiments show that the M335V mutant has significantly reduced catalytic activity (Fig. 6) even with the octanoyl-CoA substrate. Similarly, the M335A mutant also has a loss in catalytic activity (Fig. 6). The kinetic data suggest that Met-335 may be important for the catalysis by CrOT, although neither mutant displays enhanced activity with the long-chain substrates (Fig. 6).

To examine whether the mutations can disturb the conformation of the enzyme, we have determined the crystal structures of the M335V and C323M mutants at up to 2.0-Å resolution (Table I). The structural analyses demonstrate that neither mutation causes any significant changes in the structure of the enzyme (supplemental Fig. 3). As expected, the M335V mutant appears to have an enlarged acyl group binding site (Fig. 5*C*). The molecular mechanism for the reduced catalytic activity of the M335V mutant is currently not clear.

In summary, we have determined the crystal structure of mouse CrOT alone and in complex with the substrate octanoylcarnitine at up to 2.0-Å resolution. Comparison of CrOT with CrAT demonstrates how the variation of critical residues can give rise to distinctive substrate preferences within a common overall protein fold. Structure-based mutagenesis studies of CrOT and CrAT indicate that a single amino acid residue (Gly-553 in CrOT, equivalent to Met-564 in CrAT) can control the substrate preference between medium- and short-chain substrates. In contrast, our mutagenesis studies suggest that the selectivity for long-chain substrates may be determined by more complicated factors, possibly the interactions among several different residues, a detailed understanding of which will have to await the structural information on the CPTs.

Acknowledgments—We thank Randy Abramowitz and Xiaochun Yang for setting up the X4A beamline at the National Synchrotron Light Source and Farhad Forouhar, Javed Khan, Michael Rudolph, and Yang Shen for help with data collection at the synchrotron.

REFERENCES

1. Bieber, L. L. (1988) *Ann. Rev. Biochem.* **57,** 261–283
2. McGarry, J. D., and Brown, N. F. (1997) *Eur. J. Biochem.* **244,** 1–14
3. Ramsay, R. R., Gandour, R. D., and van der Leij, F. R. (2001) *Biochim. Biophys. Acta* **1546,** 21–43
4. Kerner, J., and Hoppel, C. (2000) *Biochim. Biophys. Acta* **1486,** 1–17
5. Jackson, V. N., Price, N. T., and Zammit, V. A. (2001) *Biochemistry* **40,** 14629–14634
6. Sigauke, E., Rakheja, D., Kitson, K., and Bennett, M. J. (2003) *Lab. Investig.* **83,** 1543–1554
7. Anderson, R. C. (1998) *Curr. Pharm. Des.* **4,** 1–16
8. Giannessi, F., Chiodi, P., Marzi, M., Minetti, P., Pessotto, P., de Angelis, F., Tassoni, E., Conti, R., Giorgi, F., Mabilia, M., Dell'Uomo, N., Muck, S., Tinti, M. O., Carminati, P., and Arduini, A. (2001) *J. Med. Chem.* **44,** 2383–2386
9. Wagman, A. S., and Nuss, J. M. (2001) *Curr. Pharm. Des.* **7,** 417–450
10. Thupari, J. N., Landree, L. E., Ronnett, G. V., and Kuhajda, F. P. (2002) *Proc. Natl. Acad. Sci. U. S. A.* **99,** 9498–9502
11. Thupari, J. N., Kim, E.-K., Moran, T. H., Ronnett, G. V., and Kuhajda, F. P. (2004) *Am. J. Physiol.* **287,** E97–E104
12. Farrell, S. O., and Bieber, L. L. (1983) *Arch. Biochem. Biophys.* **222,** 123–132
13. Ferdinandusse, S., Mulders, J., Ijlst, L., Denis, S., Dacremont, G., Waterham, H. R., and Wanders, R. J. A. (1999) *Biochem. Biophys. Res. Commun.* **263,** 213–218
14. Farrell, S. O., Fiol, C. J., Reddy, J. K., and Bieber, L. L. (1984) *J. Biol. Chem.* **259,** 13089–13095
15. Ramsay, R. R. (1999) *Am. J. Med. Sci.* **318,** 28–35
16. Jogl, G., and Tong, L. (2003) *Cell* **112,** 113–122
17. Ramsay, R. R., and Naismith, J. H. (2003) *Trends Biochem. Sci.* **28,** 343–346
18. Wu, D., Govindasamy, L., Lian, W., Gu, Y., Kukar, T., Agbandje-McKenna, M., and McKenna, R. (2003) *J. Biol. Chem.* **278,** 13159–13165
19. Govindasamy, L., Kukar, T., Lian, W., Pedersen, B., Gu, Y., Agbandje-McKenna, M., Jin, S., McKenna, R., and Wu, D. (2004) *J. Struct. Biol.* **146,** 416–424
20. Cai, Y., Cronin, C. N., Engel, A. G., Ohno, K., Hersh, L. B., and Rodgers, D. W. (2004) *EMBO J.* **23,** 2047–2058
21. Leslie, A. G. W., Moody, P. C., and Shaw, W. V. (1988) *Proc. Natl. Acad. Sci. U. S. A.* **85,** 4133–4137
22. Hsiao, Y.-S., Jogl, G., and Tong, L. (2004) *J. Biol. Chem.* **279,** 31584–31589
23. Cordente, A. G., Lopez-Vinas, E., Vazquez, M. I., Swiegers, J. H., Pretorius, I. S., Gomez-Puertas, P., Hegardt, F. G., Asins, G., and Serra, D. (2004) *J. Biol. Chem.* **279,** 33899–33908
24. Hendrickson, W. A., Horton, J. R., and LeMaster, D. M. (1990) *EMBO J.* **9,** 1665–1672
25. Otwinowski, Z., and Minor, W. (1997) *Method Enzymol.* **276,** 307–326
26. Weeks, C. M., and Miller, R. (1999) *J. Appl. Crystallogr.* **32,** 120–124
27. Sheldrick, G. M. (1990) *Acta Crystallogr. Sect. A* **46,** 467–473
28. Terwilliger, T. C., and Berendzen, J. (1999) *Acta Crystallogr. Sect. D Biol. Crystallogr.* **55,** 849–861
29. Jones, T. A., Zou, J. Y., Cowan, S. W., and Kjeldgaard, M. (1991) *Acta Crystallogr. Sect. A* **47,** 110–119
30. Brunger, A. T., Adams, P. D., Clore, G. M., DeLano, W. L., Gros, P., Grosse-Kunstleve, R. W., Jiang, J.-S., Kuszewski, J., Nilges, M., Pannu, N. S., Read, R. J., Rice, L. M., Simonson, T., and Warren, G. L. (1998) *Acta Crystallogr. Sect. D Biol. Crystallogr.* **54,** 905–921
31. Ramsay, R. R., Derrick, J. P., Friend, A. S., and Tubbs, P. K. (1987) *Biochem. J.* **244,** 271–278
32. Hendrickson, W. A. (1991) *Science* **254,** 51–58
33. Mattevi, A., Obmolova, G., Schulze, E., Kalk, K. H., Westphal, A. H., de Kok, A., and Hol, W. G. J. (1992) *Science* **255,** 1544–1550
34. Chothia, C., and Lesk, A. M. (1986) *EMBO J.* **5,** 823–826
35. Cronin, C. N. (1997) *Biochem. Biophys. Res. Commun.* **238,** 784–789
36. DeLano, W. L. (2002) *Pymol*, DeLano Scientific, San Carlos, CA

Downloaded from www.jbc.org by on August 19, 2006